Miniature temperature sensor based on optical microfiber

Zhengtong Wei (卫正统), Zhangqi Song (宋章启)*, Xueliang Zhang (张学亮), Yang Yu (于 洋), and Zhou Meng (孟 洲)

College of Optoelectronic Science and Engineering, National University of Defense Technology, Changsha 410073, China

**Corresponding author: songzhangqi@nudt.edu.cn*

Received June 27, 2013; accepted September 4, 2013; posted online November 4, 2013

Optical microfibers (OMs) are good alternatives in the field of sensing. In this letter, a simple and effective miniature temperature sensor based on OM is proposed and experimentally verified. Using pure water and fiber coating as the OM clad, an additional loss will occur due to the absorption of outer medium. The temperature of the outer environment can be estimated by monitoring the change in additional loss. In the demonstrated experiments, a series of OM with different diameters, waist lengths, and constructions are used as sensing elements. The correlation coefficients between the experimental results and the linear fittings are better than 0.99, and the temperature sensitivity obtained by the linear fittings can achieve –0.151 dB/°C (in pure water) and –0.405 dB/°C (covered by fiber coating). Moreover, higher sensitivity can be obtained by decreasing the diameter, increasing the waist length of the OM, or choosing the proper operating wavelength.

OCIS codes: 060.2370, 060.2300, 060.4005.
doi: 10.3788/COL201311.110602.

Temperature is an important physical parameter that should be accurately determined in many contexts[1], such as in environmental measurement, chemical industry, and remote sensing. Temperature sensors based on optical fiber have been widely developed because of their immunity to electromagnetic interference and possibility to work in contact with explosives[2]. Fiber Bragg gratings (FBGs) are the most popular sensing elements for temperature measurement[3]; however, cross-sensitivity is a key challenge of FBG applications[4]. Numerous studies have been conducted to solve such problem[5−8], but the process and construction are more complicated.

Optical microfiber (OM) has been extensively researched because of the enormous progress in the fabrication of low-loss structures that allow for low-loss evanescent wave guiding[9,10]. In the sensing field, OM has distinct advantages because of its enabling optical properties, including large evanescent fields, high-nonlinearity, strong confinement, large waveguide dispersion, and small bending radius. When light is transmitted in the OM, a relatively large fraction of the guided power propagates out of the physical boundary as an evanescent field, making it highly sensitive to the outer medium. OM has been successfully used to sense humidity[11], refractive index[12,13], gas concentration[14], current[15], micro particle[16], and temperature[17−24]. The temperature sensor in Refs.[17-21] obtains the parameter by using an optical spectrum analyzer (OSA) and by monitoring the shift of interference fringe, which makes the whole system expensive and unpractical. Meanwhile, temperature is measured by recording the change of peak reflected wavelength[22−24]; however, the fabrication of FBG in OM (MFBG) is difficult and complicated.

In this letter, a miniature temperature sensor based on OM is proposed and demonstrated. The sensing OM is used as a sensing element and a transmission channel. After OM fabrication, the profile is surrounded by materials with lower refractive index and absorption coefficient, such as pure water and optical fiber coating. The absorption coefficient of the outer-surrounding material changes due to the change in temperature, thereby inflecting the transmitted power. Temperature can be estimated by monitoring the additional loss. The proposed sensor has the advantages of conventional optical fiber temperature sensor, as well as the characteristics of ultra compactness, high resolution, good repeatability, simple construction, and easy operation.

The sensing OMs used in this letter were fabricated from conventional single-mode fiber (SMF) by modified flame-brush method[9]. The heat intensity can be controlled to ensure a sufficiently high temperature to soften the SMF by adjusting the micro-heater current. OMs with different diameters can be fabricated by controlling the taper-drawing speed. To demonstrate the facility of our proposal, two kinds of materials were used as the outer medium in our demonstration experiments.

When the fabricated OM is surrounded by lower refractive index material (such as pure water and optical fiber coating), a two-layer waveguide consisting of the core and the outer surrounding is composed. A relatively large fraction power is propagated in the outer medium due to the ultra-tiny scale of OM. Moreover, a fraction of the power transmitted in the clad can be calculated by

$$\eta = \frac{\int_a^{\infty} S_{z2} \mathrm{d}A}{\int_0^a S_{z1} \mathrm{d}A + \int_a^{\infty} S_{z2} \mathrm{d}A}, \tag{1}$$

where a is; OM radius; S_{z1} and S_{z2} represent the z-components of the Poynting vectors in the OM and the clad (surrounding medium), respectively[25]. If the outer material is pure water and the core is silica (in this letter, OM is fabricated from silica), a fraction of the power transmitted in the outer diameter can be obtained, as shown in Fig. 1.

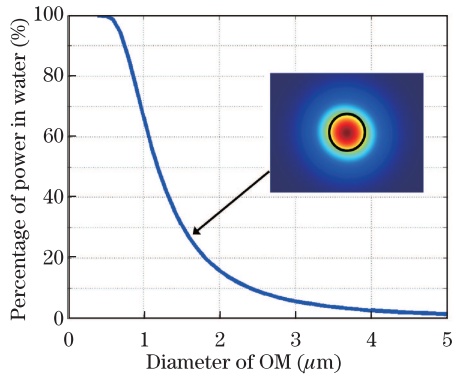

Fig. 1. Percentage of the power transmitted in the water verse diameter of OM. The inset shows the result obtained by COMSOL software for OM, with diameter of 1.5 μm (the refractive indexes of the OM and water are 1.451 and 1.316, respectirely, whereas the light wavelength is 1.55 μm).

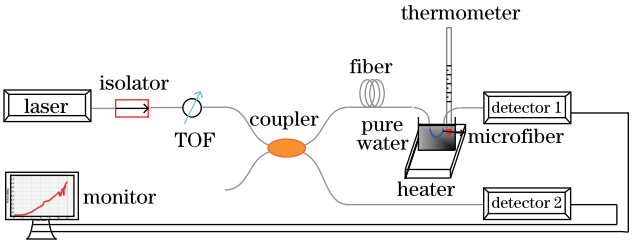

Fig. 2. Schematic of the temperature-sensing experiment using pure water.

Part of the power transmitted in the water increases with the decrease in OM diameter, as shown in Fig. 1. An additional loss will occur[26] when the OM is surrounded by water due to the absorption function of water. When the temperature of the outer environment changes, the absorption coefficient of the water changes accordingly[27,28], thereby inflecting additional loss. Temperature can be estimated by monitoring the change in additional loss.

The additional loss of the OM due to temperature change is measured with an optical fiber loss measurement system, as shown in Fig. 2. A laser (RIO) with 1.55-μm wavelength is used as the source. The light of the source splits into two beams. One is injected into the measured OM and immersed into pure water laid on a current-driven heater. The transmitted power is then measured with a detector (OE-200-IN2-FC). The other beam is tested with another detector (OE-200-IN2-FC) to cancel the power fluctuation of the source. The temperature of the tested pure water is measured by a thermometer during the experiments. The pure water used in our experiments is strictly purified by a commercial purity machine and tested by monitoring the resistance.

In the experiments, two OMs with diameters of 1.7 and 2.4 μm are tapered. Their waist lengths are 10 mm, and the relative rate of the hot-zone change and taper elongation (α) is 0.2[29]. By setting these OMs as the sensing head and heating the pure water, the experimental data between the temperature of pure water and the additional loss of OM is obtained. The results obtained by the two OMs are both plotted and linearly fitted in Fig. 3.

The additional losses are basically linear with the temperature of pure water, and the additional loss for the 1.7-μm diameter OM is larger than that for the 2.4 μm, as shown in Fig. 3. The first- and second-degree polynomial fitting results between the additional loss and the temperature for the 2.4-μm OM are both calculated. The correlation coefficients between the experimental and fitting results are 0.9989 and 0.9996, respectively. Compared with the first-degree polynomial fitting results, the second-degree polynomial fitting results are slightly more precise. The nonlinear behavior is due to the interplay of the refractive index changes of both fiber and outer medium[24]. However, the working principle and the temperature regions are different from those in Ref. [24], and the experimental results do not show obvious nonlinear behavior. Moreover, the first-order polynomial coefficient (0.046) is about five hundred times larger than that of the second order (0.000099). Thus, only first-degree polynomial fitting has been carried out in the sensing temperature regions in the following text, whereas the first-order polynomial coefficient of the linear fitting is only the sensitivity of the OM.

The sensitivity of the 1.7-μm diameter OM (–0.083 dB/°C) obtained by linear fitting is higher than that of the 2.4-μm diameter OM (–0.038 dB/°C). The background noise of the whole system has been tested to be lower than 0.005 dB, so the minimum detectable temperature variation is 0.06 °C for the 1.7-μm diameter OM and 0.13 °C for the 2.4-μm OM. When higher sensitivity is needed, thinner diameter and longer waist length OM can be used.

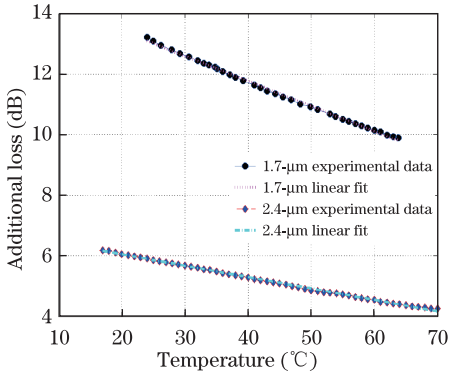

Fig. 3. Additional loss of OM changes with the heating process of pure water.

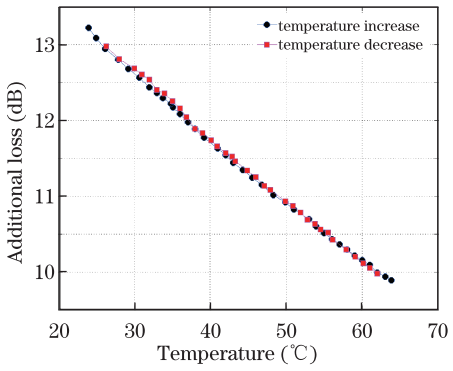

Fig. 4. Additional loss obtained during the heating and cooling processes of water (1.7-μm diameter OM).

To demonstrate the repeatability of the temperature sensor, the additional loss during the heating and cooling processes are both recorded for the 1.7-μm diameter OM, as shown in Fig. 4. The additional loss for pure water heating from 23 to 64 °C (warm up by heater, takes several minutes) and that for water cooling from 62 to 29 °C (natural cooling, takes hours) are both shown in Fig. 4. The experimental results display good repeatability.

The absorption coefficient usually changes with temperature and operating wavelength; thus, temperature experiments with different operating wavelengths are carried out. An OM with a diameter of 1.6 μm and a waist length of 12 mm, as well as an OM with a 2.35-μm diameter and a 10-mm waist length, are set as the sensing head. The α for both OMs are 0.2. In the experiments, a tunable fiber laser (Nett est) is used as the source, and the additional loss for different wavelengths are measured at the same temperature, as shown in Fig. 5.

The additional losses vary with different wavelengths due to the difference in absorption coefficient. The additional loss linearly decreases with the increase in temperature, and the correlation coefficients between the experimental results for different wavelengths and linear fittings are above 0.998. The sensitivity for different operating wavelengths obtained by linear fitting is shown in Fig. 6.

Figure 6 shows that the temperature sensitivity for the shorter wavelength in the experiments is larger than that of the longer wavelength, and the sensitivity for the OM with thinner diameter is larger than that with thicker diameter, as shown in Fig. 3. Thus, in actual application, higher sensitivity can be achieved by decreasing the OM diameter and choosing the proper operating wavelength.

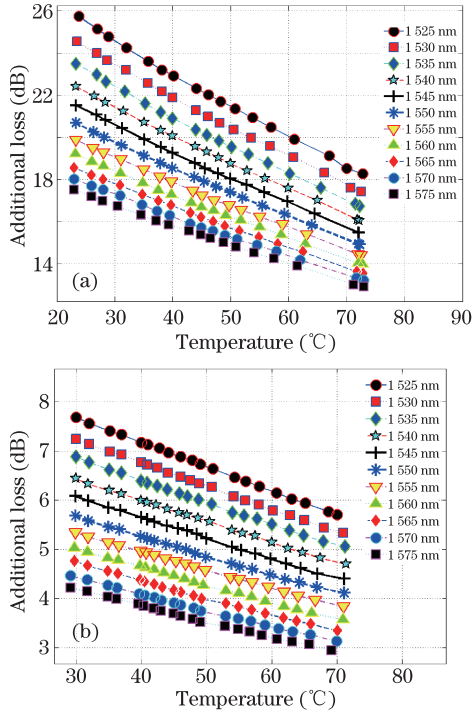

Fig. 5. Additional loss changes with temperature of water for different wavelengths. (a) Result for the 1.6-μm diameter OM; (b) result for the 2.35-μm diameter OM.

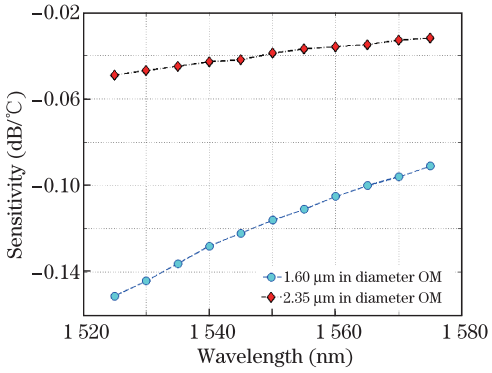

Fig. 6. Sensitivity changes with the operating wavelength for different OM diameters.

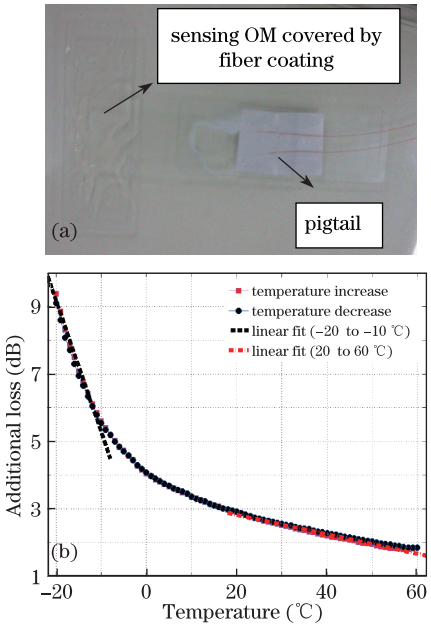

Fig. 7. (a) Photograph of the sensing OM covered by fiber coating; (b) additional loss obtained during the heating and cooling processes (2.1-μm diameter OM covered by fiber coating).

Similar experiments have been carried out using fiber coating as surrounding medium. The fiber coating is fabricated by The North Coating Research Central in China. The refractive index of the fiber coating is about 1.42, which can be used in the range of –60 to 200 °C. An OM with a diameter of 2.1 μm and a waist length of 10 mm is set as the sensing head and covered by fiber coating, with α of 0.1. After embedding the sensing OM into the fiber coating and curing with ultraviolet light for about 30 s, a 3-dB additional loss occurs due to the absorption. The photograph of the sensing OM covered by fiber coating is shown as Fig. 7(a). A laser (RIO) with 1.55-μm wavelength is used as the source, and the whole sensing OM covered by fiber coating is laid in an oven with temperature ranging from –40 to 80 °C. Additional loss for different temperatures can be measured by setting the temperature heating and cooling in the range of –20 to 60 °C.

The sensing OM covered by the fiber coating has good temperature repeatability, as shown in Fig. 7(b). When

the temperature changes in the range from –10 to –20 °C, the temperature sensitivity of the sensing OM is about –0.405 dB/°C, whereas the temperature goes to the range of 20 – 60 °C and the sensitivity is about –0.034 dB/°C. The correlation coefficients between the experimental results and the linear fittings are both better than 0.99 in the mentioned temperature regions. Thus, the sensing OM covered by this kind of fiber coating is more sensitive to low temperature. The background noise of the system is lower than 0.005 dB.

In conclusion, a temperature sensor based on OM is proposed and demonstrated. When the fabricated OM is surrounded by pure water or fiber coatings, an additional loss will occur due to the absorption of the outer medium. In addition, the absorption coefficient changes with temperature, leading to additional loss. Thus, the temperature can be estimated by monitoring the additional loss of the sensing OM. The experimental results show good repeatability, and lower than 0.1 °C temperature variation can be measured. The temperature sensing range depends on the outer medium, wherein potentially high temperature and low temperature can be tested if the proper material is chosen. Two methods can be used to further improve the sensor sensitivity. Firstly, the diameter of the OM can be decreased and the waist length can be increased. Secondly, the operating wavelength can be optimized. The temperature sensor has the following characteristics: ultracompactness, high resolution, good repeatability, simple construction, and easy operation. In addition, the sensor can be used for studying the temperature characteristic of material absorption. However, due to the limitation imposed by the refractive index of silica and the working principle of the sensor, only the material with refractive index lower than 1.45 and the absorption coefficient can be used as the surrounding material. Future work will be focused on the proper package for the temperature sensor.

References

1. B. Culshaw and A. Kersey, J. Lightwave Technol. **26,** 1064 (2008).
2. K. T. V. Grattan and B. T. Meggitt, *Optical Fiber Sensor Technology* (Kluwer Academic Publishers, Boston, 2000).
3. V. de Oliveira, M. Muller, and H. J. Kalinowski, Appl. Opt. **50,** E55 (2011).
4. S. E. Kanellopoulos, V. A. Handerek, and A. J. Rojers, Opt. Lett. **20,** 333 (1995).
5. A. Quintela, L. Rodriguez, M. I. Barquin, C. Galindez, M. A. Quintela, and J. M. Lopez-Higuera, Proc. SPIE **7753,** 77537G (2012).
6. H. F. Lima and, P. F. Antunes, J. de Lemos Pinto, and R. N. Nogueira, IEEE Sens. J. **10,** 269 (2010).
7. D. Viegas, S. Abad, J. L. Santos, L. A. Ferreira, and F. M. M. Araújo, IEEE Photon, Technol. Lett. **22,** 811 (2010).
8. W. Urbanczyk, E. Chmielewska, and W. J. Bock, Meas. Sci. Technol. **12,** 800 (2001).
9. G. Brambilla, J. Opt. **12,** 043001 (2010).
10. F. Xu, G. Brambilla, J. Feng, and Y.-Q. Lu, IEEE Photon. Technol. Lett. **22,** 218 (2010).
11. L. Zhang, F. Gu, J. Lou, X. Yin, and L. Tong, Opt. Express **16,** 13349 (2008).
12. H. Zhu, Y. Wang, and B. Li, ACS Nano **3,** 3110 (2009).
13. Q. Liu and Q. Wang, Chin. Opt. Lett. **10,** 090601 (2012).
14. M. Tonezzer and R. G. Lacerda, Sensor Actuator B Chem. **150,** 517 (2010).
15. M. Belal, Z. Song, Y. Jung, G. Brambilla, and T. P. Newson, Opt. Lett. **35,** 3045 (2010).
16. Z. Wei, Z. Song, X. Zhang, and Z. Meng, IEEE Photon. Technol. Lett. **25,** 568 (2013).
17. Y. Wu, Y. Rao, Y. Chen, and Y. Gong, Opt. Express **17,** 18142 (2009).
18. Y. Wu, L. Jia, T. Zhang, Y. Rao, and Y. Gong, Opt. Commun. **285,** 2218 (2012).
19. N. Díaz-Herrera, M. C. Navarrete, O. Esteban, and A. González-Cano, Meas. Sci. Technol. **15,** 353 (2004).
20. M. Ding, P. Wang, and G. Brambilla, IEEE Photon. Technol. Lett. **24,** 1209 (2012).
21. Y. Zhang, W. Zou, X. Li, J. Mao, W. Jiang, and J. Chen, Chin. Opt. Lett. **10,** 070609 (2012).
22. J.-L. Kou, S.-J. Qiu, F. Xu, and Y.-Q. Lu, Opt. Express **19,** 18452 (2011).
23. Y. Ran, L. Jin, L.-P. Sun, J. Li, and B.-O. Guan, Opt. Lett. **37,** 2649 (2012).
24. R. C. Kamikawachi, I. Abe, H. J. Kalinowski, J. L. Fabris, and J. L. Pinto, IEEE Sensors J. **7,** 1358 (2007).
25. L. Tong, J. Lou, and E. Mazur, Opt. Express **12,** 1025 (2004).
26. Z. Wei, Z. P. Song, X. Zhang, and Z. Meng, Proc. SPIE **8421,** 8421183 (2012).
27. D. T. Kunde, V. Danicke, M. Wendt, and R. Brinkmann, IFMBE Proc. **22,** 2228 (2008).
28. E. D. Jansen, T. G. van Leeuwen, M. Motamedi, C. Borst, and A. J. Welch, Laser Surg. Med. **14,** 258 (1994).
29. T. A. Birks and Y. W. Li, J. Lightwave Technol. **10,** 432 (1992).